International Biodeterioration & Biodegradation 208 (2026) 106274

Contents lists available at ScienceDirect

International Biodeterioration & Biodegradation

journal homepage: www.elsevier.com/locate/ibiod

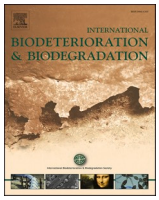

Biofilm-mediated mitigation of nitrous oxide emissions in anammox-based wastewater treatment

Zhiman Lin [a,1], Jinfan Zhang [a,1], Ru Wang [a], Jingmin Ou [a], He Zhang [a], Zihua Wang [a], Fangyuan Zheng [a], Xiantao Sun [a], Xin Wei [a], Yiming Huang [a], Zhenguo Chen [c,d], Mark C.M. van Loosdrecht [b], Yuchun Yang [a,*]

[a] State Key Laboratory of Biocontrol, School of Ecology, Shenzhen Campus of Sun Yat-sen University, Shenzhen, Guangdong, 518107, China
[b] Delft University of Technology, Department of Biotechnology, van der Maasweg 9, 2629, HZ Delft, the Netherlands
[c] Guangdong Provincial Engineering Research Center of Intelligent Low-carbon Pollution Prevention and Digital Technology, South China Normal University, SGuangzhou, 510006, China
[d] SCNU (NAN'AN) Green and Low-carbon Innovation Center, Nan'an SCNU Institute of Green and Low-carbon Research, Quanzhou, 362300, China

ARTICLE INFO

Keywords:
Anammox
Nitrous oxide
Biofilm
Sustainable wastewater treatment

ABSTRACT

Wastewater treatment is a major source of global greenhouse gas (GHG) emissions, largely driven by nitrous oxide (N_2O) release during nitrogen removal processes. While anaerobic ammonium-oxidizing (anammox) bacteria have become widely adopted to optimize nitrogen removal, the pathways governing N_2O emissions in anammox systems remain insufficiently characterized. Findings revealed that in aerobic environments with low dissolved oxygen, nitrifying microorganisms showed pronounced upregulation of N_2O synthesis genes, confirming their pivotal role in emissions. Conversely, heterotrophic denitrification dominated N_2O production in anaerobic systems. Crucially, anammox-dominated biofilms displayed substantially lower expression of N_2O-related genes compared to suspended sludge, suggesting reduced emission risks in biofilm configurations. Batch experiments demonstrated a 2.78-fold lower N_2O release from biofilms than suspended biomass. This mitigation was linked to restricted substrate transport within biofilms, which curbed NO_2^- buildup and subsequently suppressed nitrifier-derived N_2O formation. Additionally, the high-density colonization of anammox bacteria in biofilms efficient scavenging of nitric oxide (NO) and hydroxylamine (NH_2OH), critical intermediates in N_2O synthesis. Employing an integrated multi-omics approach, this study investigates N_2O production and consumption pathways in diverse anammox systems and unveils the N_2O mitigation mechanisms of biofilms, offering fundamental insights for reducing N_2O emissions in wastewater treatment.

1. Introduction

Nitrous oxide (N_2O), a potent greenhouse gas (GHG) with a global warming potential (GWP) 298 times higher than CO_2 (Eggleston and Buendia, 2006), ranks as the third most significant GHG after carbon dioxide (CO_2) and methane (CH_4). Atmospheric N_2O concentrations have risen steadily at an average annual rate of ~0.31 % over the past decade (Rajendra et al., 2014). Wastewater treatment systems contribute to up to 25 % of global GHG emissions (Kyung et al., 2015), with biological nitrogen removal processes accounting for up to 80 % of these emissions (Wu et al., 2020). These findings highlight the critical need to develop N_2O mitigation strategies for sustainable wastewater treatment technologies.

Anaerobic ammonia oxidation (anammox, AMX) offers a streamlined pathway in the nitrogen cycle, bypassing the need for conventional nitrification/denitrification by directly converting ammonium (NH_4^+) and nitrite (NO_2^-) to nitrogen gas (N_2) (Lackner et al., 2014; Liang et al., 2025). Owing to its energy efficiency, anammox has emerged as a key technology for treating ammonium-rich wastewater, with configurations such as single- and two-stage partial nitrification/anammox (PNA) (Lackner et al., 2014), partial denitrification/anammox (PDA) (Wu et al., 2020), and simultaneous nitrification/anammox/denitrification (SNAD). By 2014, over 200 full-scale wastewater treatment plants (WWTPs) had adopted anammox-based systems, and adoption continues

* Corresponding author.
E-mail address: yangych55@mail.sysu.edu.cn (Y. Yang).
[1] Authors contributed equally to this work.

https://doi.org/10.1016/j.ibiod.2025.106274
Received 24 October 2025; Accepted 28 December 2025
Available online 31 December 2025

to expand globally (Cao et al., 2017).

N_2O emissions in these systems stem primarily from three microbial pathways: nitrification, nitrifier denitrification, and heterotrophic denitrification (Ma et al., 2017). While denitrifying bacteria uniquely mitigate N_2O reduction by reducing it to N_2 (Lin et al., 2022), the coexistence of nitrifying and denitrifying microorganisms in anammox systems can drive substantial N_2O production through these pathways, posing a major challenge to sustainable implementation (Wu et al., 2020; Lin et al., 2022). A critical advantage of anammox bacteria lies in their natural propensity to form dense aggregates, enabling their enrichment in biofilms or granular sludge (Fernández et al., 2008; Wu et al., 2020; Lin et al., 2022; Zhang et al., 2023). These biomass retention strategies-attached biofilms and suspended granules-enhance process stability under fluctuating conditions and are central to mainstream anammox technologies (Chen et al., 2022; Wang et al., 2022). Despite extensive research on optimizing nitrogen removal and broadening application scenarios, N_2O emissions remain poorly understood, undermining efforts to develop effective mitigation strategies. The mechanisms and potential for N_2O emissions differ significantly between biofilms and suspended sludge. A key driver is substrate mass transfer limitation within biofilms, which directly affects microbial processes (He et al., 2023a; Hong et al., 2025). Consequently, these metabolic differences contribute to the establishment of distinct microbial communities. We therefore hypothesis that divergent N_2O emission potentials stem largely from differences in the abundance and activity of N_2O consuming microbes between the two sludge types.

In this study, metagenomic and metatranscriptomic analyses were applied to various anammox-driven wastewater treatment systems using eight widely used nitrogen removal technologies. By combining nitrogen cycle gene profiles with metatranscriptomic data, we reconstructed the intricate N_2O metabolic networks driven by microbial functional groups within these systems. Furthermore, batch cultivation in a single-stage PNA reactor were employed to evaluate the N_2O production dynamics of two biomass growth forms: suspended sludge versus attached biofilm. To our knowledge, this study provides the first comprehensive analysis of microbial nitrogen cycling pathways and N_2O emission mechanisms across multiple anammox-based systems, validated through biochemical batch cultivation experiments.

2. Materials and methods

2.1. Global metagenomic and metatranscriptomic data collection

Publications reporting metagenomic and metatranscriptomic analyses of anammox-driven wastewater treatment systems were retrieved from Google Scholar (https://scholar.google.com) and Web of Science (https://www.webofscience.com) on February 8, 2023, using the search query: *TS = "anammox AND metagenome AND metatranscriptome"* (Xu et al., 2025; Xu et al., 2025). Studies were filtered based on the following criteria: (1) published in English in Science Citation Index (SCI)-indexed journals, (2) anammox-driven reactors operated for ≥3 months, and (3) availability of both metagenomic and metatranscriptomic raw data in public repositories. Thirteen articles meeting these criteria were selected (Fig. 1). Key operational and physicochemical parameters—including aggregate type (suspended sludge or attached biofilm), reactor configuration (sole anammox, PNA, SNAD, or PDA), dissolved oxygen (DO), pH, influent NH_4^+, NO_2^- and nitrate (NO_3^-), and carbon-to-nitrogen (C/N) ratio—were extracted from the selected studies.

All metagenomic and metatranscriptomic data were download from the NCBI Sequence Read Archive (SRA). Raw SRA files were converted to FASTQ format using the fasterq-dump tool in sra-tools (https://github.com/ncbi/sra-tools). Raw reads were quality-filtered and trimmed using the Read_QC module of metaWRAP v1.3.2 with the default settings (Uritskiy et al., 2018). For metatranscriptomic data, residual ribosomal RNA (rRNA) sequences were removed using SortMeRNA v4.3.7 with the SILVA 138 SSURef NR99 database as the reference (Kopylova

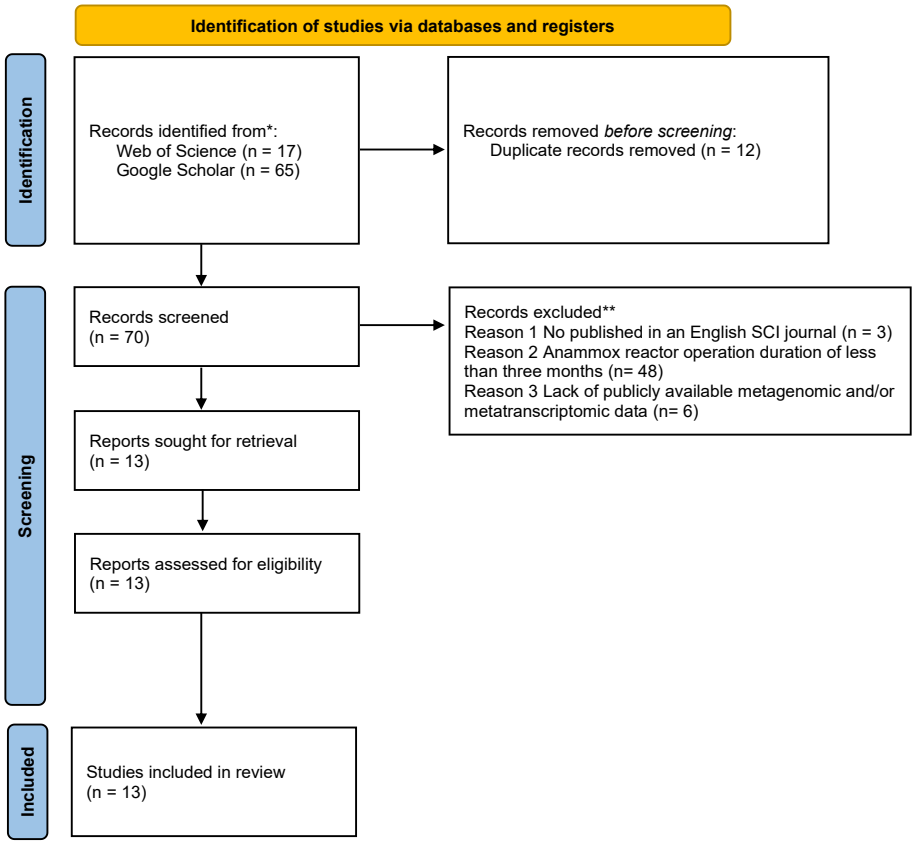

Fig. 1. PRISMA flow diagram for systematic review.

et al., 2012). Metagenomic assemblies were constructed de novo using the metaWRAP (v1.3.2) pipeline with the metaSPAdes assembler, retaining contigs longer than 1000 bp. Metagenome assembled genomes (MAGs) were subsequently reconstructed with Metabat2 (v2.0) (Kang et al., 2015), CONCOCT (v1.0.0) (Alneberg et al., 2014), and MaxBin2 (v2.0) (Wu et al., 2016) using contigs longer than 1500 bp. Only MAGs with >50 % completeness and <10 % contamination were retained for downstream phylogenomic analysis. Open reading frames (ORFs) were predicted from assembled scaffolds and MAGs using Prodigal (v2.6.3) (Hyatt et al., 2010). Trimmed metagenomic and metatranscriptomic reads were aligned to assembled contigs and predicted ORFs using Bowtie2 (v2.3.5.1) (Langmead and Salzberg, 2012). Gene and transcript abundances were quantified via the covern conting using CoverM (v0.6.1) (https://github.com/wwood/CoverM) from metagenomic and metatranscriptomic alignments, respectively. To enable cross-sample comparisons, read counts were normalized as CPM (Counts Per Million) for metagenomic data and TPM (Transcripts Per Millon) for metatranscriptomic data, ensuring that the sum of normalized values per sample equals one million (Segata et al., 2012; Debeljak et al., 2023).

2.2. Genome de-replication and taxonomic analysis

The completeness and contamination of all recovered MAGs were assessed using CheckM v1.0.6 (Parks et al., 2015). Species-level clustering was performed with dRep v3.2.0 (Olm et al., 2017) using an average nucleotide identity (ANI) threshold of 95 % (-pa 0.95 option) (Konstantinidis and Tiedje, 2005). Resulting species-level genome operational taxonomic units (gOTUs) were retained for downstream analyses. Taxonomic classification of filtered MAGs was assigned using GTDB-Tk v2.3.2 (Chaumeil et al., 2020) with the GTDB reference database (release R214). A phylogenomic tree was reconstructed with IQ-TREE (Nguyen et al., 2015) using 43 marker genes identified by CheckM (default parameters) and visualized in iTOL (Letunic and Bork, 2019).

2.3. Construction of nitrogen cycle networks and N_2O metabolisms pathways

Custom protein databases for N_2O-related enzymes—cytochrome P460 (CytL), copper-containing nitrite reductase (NirK), and nitric oxide reductase (NorB)—were constructed using 99 published ammonia-oxidizing bacteria (AOB) genomes (Supplementary Table 1). Representative sequences were retrieved via BLASTP (E-value $<10^{-10}$) against NCBI RefSeq and UniProtKB/Swiss-Prot, followed by phylogenetic validation with IQ-TREE (default settings) (Nguyen et al., 2015). Sequence clustering at 90% identity was performed using USEARCH v8.1.186 (Forster et al., 2016), with representative sequences compiled into databases via NCBI's makeblastdb.

The predicted protein then functionally annotated using BLASTP against both a previously published nitrogen cycle gene database (Yang et al., 2020) and a newly built CytL, NirK, and NorB databases. The initial hits were filtered using an E-value cutoff of $<10^{-10}$, a minimum amino acid identity of 60 %, and a query coverage of >50 %. Curated sequences were incorporated into functional gene databases to reconstruct nitrogen cycle networks, integrating gene abundance and transcript levels. Spearman correlations between physicochemical parameters and nitrogen cycle genes were calculated using R packages corrplot and dplyr, while Mantel tests (via http://mem.rcees.ac.cn:8080) evaluated linkages among gene expression, nitrogen transformation processes, and operational variables.

2.4. Phylogenetic analyses of key functional genes

Hydrazine synthase (HZS), ammonium monooxygenase (AMO), NirK, heme-containing nitrite reductase (NirS), nitric oxide reductase (NorB), and nitrous oxide reductase (NosZ) sequences retrieved from assemblies were aligned using MAFFT (Yamada et al., 2016), followed by trimming of ambiguous regions with trimAl with the setting '-gt 0.1' (Capella-Gutiérrez et al., 2009). Unrooted maximum-likelihood phylogenetic trees were reconstructed using IQ-TREE v2.2.0.3 (Nguyen et al., 2015), with modelFinder (Kalyaanamoorthy et al., 2017) for best-fit substitution model selection and UFboot2 (Hoang et al., 2018) (1000 replicates) for branch support estimation. Gene sequences were taxonomically classified via BLASTP against the NCBI RefSeq protein database (E-value $<10^{-10}$ and ≥95 % species-level identity). Final trees were annotated and visualized in iTOL (Letunic and Bork, 2019).

2.5. Single-stage PNA reactor setup and operation

A 5-L single-stage PNA reactor (10 cm diameter × 60 cm height) was constructed, with anammox-enriched activated sludge from a landfill leachate treatment plant serving as the inoculum in the bottom compartment. Seventy-five-centimeter flexible fiber bundles were suspended in the upper section to facilitate biofilm attachment. Hydraulic retention time (HRT) was maintained at 24 h via continuous feeding of synthetic ammonium-rich wastewater containing (per liter): 6 mM of NH_4Cl, 6 mM of $NaNO_2$, 1 g L^{-1} of $NaHCO_3$, 27.2 mg L^{-1} of K_2HPO_4, 300 mg L^{-1} of $MgSO_4$, 180 mg L^{-1} of $CaCl_2$ and 1 mL of trace element stock solution. The trace element stock solution comprised (per liter): 0.43 $ZnSO_4.7H_2O$, 0.24 $CoCl_2{\cdot}6H_2O$, 0.99 $MnCl_2{\cdot}4H_2O$, 0.25 $CuSO_4{\cdot}5H_2O$, 0.22 $Na_2MoO_4{\cdot}2H_2O$, 0.19 $NiCl_2{\cdot}6H_2O$, 0.014 H_3BO_3, 5 $FeSO_4{\cdot}2H_2O$ and 5 EDTA.

2.6. Microbial community analysis

Suspended sludge and attached biofilm samples were collected from the PNA reactor after 740 days of stable operation. Total genomic DNA was extracted from both biomass types using the PowerSoil DNA Isolation Kit (QIAGEN, Germany) following manufacturer protocols. DNA concentration was quantified with a Nanodrop spectrophotometer (Thermo Fisher Scientific, USA) and stored at −80 °C until processing. 16S rRNA gene amplicon sequencing targeting the V4 hypervariable region (primers 515f: GTGCCAGCMGCCGCGGTAA; 806r: GGACTACHVGGGTWTCTAAT) (Huws et al., 2007) was conducted by Guangdong Magigene Technology Co., Ltd. (China). Sequencing was performed on the Illumina NovaSeq 6000 platform, which yielded approximately 60,000 raw paired-end reads (2 × 300 bp). Raw sequencing reads were processed and denoised using QIIME 2 (Caporaso et al., 2010). Briefly, demultiplexed reads were set as follows: -p-trim--left-f 18 and –p-trim-left-r 20 to remove the 515F and 806R primer sequences, respectively; –p-trunc-len-f 0 and –p-trunc-len-r 0 for no truncation; –p-max-ee 5.0 for quality filtering; and –p-min-overlap 20 to enable merging. Amplicon sequence variants (ASVs) were inferred through a process of denoising and error correction with the DADA2 algorithm. This method corrects Illumina-sequenced amplicon errors to infer true biological sequences, providing single-nucleotide resolution. The analysis was performed using the dada2 denoise-paired command in QIIME 2. Representative sequences from each ASV were aligned against the SILVA v138 SSU rRNA reference database (Quast et al., 2013) for taxonomic classification.

2.7. Batch cultivation experiments on N_2O production

Batch experiments quantified N_2O production rates from suspended sludge versus attached biofilm in the single-stage PNA reactor after two years of stable operation. Triplicate biological replicates were prepared by collecting 1 L of mixed liquor (suspended sludge) and 15-cm biofilm-attached flexible fiber bundles per replicate. After centrifugation, supernatants discarded, and pellets resuspended in 1.5 L of synthetic medium within 2.5-L bioreactors. Anoxic conditions were established by continuous argon (Ar) sparging (0.1 L min^{-1}) until DO reached <0.1 mg L^{-1}. Each 50-min cycle consisted of a 10 min aeration phase followed by

40 min anoxic phase, with air and Ar as 0.1 L min^{-1}, respectively, such that a low-aeration condition with a DO level of 0.7 ± 0.2 mg L^{-1} was maintained. Temperature was automatically maintained at 30 ± 1 °C with continuous mixing 80 rpm min^{-1}. The synthetic medium was performed prepared as described with ~5 mM NH_4^+ as the substrate.

Liquid samples collected every 10 min were filtered (0.22-μm membrane) and analyzed for NH_4^+, NO_3^- and NO_2^-. NH_4^+ was measured photometrically as described previously (Hood-Nowotny et al., 2010). NO_3^- was reduced to NO_2^- by vanadium chloride, and NO_2^- and NO_3^- were determined photometrically (Miranda et al., 2001). Gas-phase N_2O concentrations were quantified using a gas chromatograph (GC9790Plus, Fuli) equipped with an electron capture detector (ECD). The system was calibrated using a single-point method with certified N_2O standard gas mixture (0.289 ppmv, balanced in N_2), and the method's limit of detection (LOD) was 1×10^{-13} g mL^{-1}. The N_2O emission factor was calculated as the ratio of the total mass of N_2O emitted to the mass of removed nitrogen, based on equations (1) and (2) (He et al., 2023b).

$$m_{N_2O} = \frac{Q \cdot M_{N_2O} \cdot P}{R \cdot T} \sum_{2}^{n} \left[\frac{C_{n-1} + C_n}{2} \cdot \Delta t \right] \quad (1)$$

$$EF_{N_2O} = \frac{m_{N_2O}}{m_{TN-removal}} \quad (2)$$

where Q is the pumping gas flow rate from the reactor headspace for the N_2O concentration detection (L min^{-1}), P is the atmospheric pressure (1 atm), R is the gas constant (0.082 L atm K^{-1} mol^{-1}), T is the temperature (K), C_n is the concentration of N_2O of the collected sample (ppmv), Δt is the time interval of logged data (10 min), $m_{TN\text{-}removal}$ denoted the total mass of amount of nitrogen removal.

3. Results and discussion

3.1. Operation parameters of distinct anammox-driven systems

This global meta-analysis synthesized data from 13 genomic studies (including three prior investigations from our group) spanning 12 suspended sludge and 7 biofilm-based anammox systems (Supplementary Table 2). We systematically evaluated critical operational parameters known to influence N_2O emissions, such as DO, pH, T, NH_4^+, NO_2^-, and COD (Lin et al., 2022). DO levels ranged from 0 to 1.4 mg L^{-1}, indicating the prevalence of anaerobic or hypoxic conditions for anammox applications. The pH was maintained between 6.7 and 8.62, which aligns with the neutral to slightly alkaline conditions preferred by anammox bacteria (Oshiki et al., 2016a). Inorganic nitrogen concentrations exhibited significant variability, with NH_4^+-N levels spanning 25–462 mg L^{-1}, NO_2^--N ranging from 0 to 424.8 mg L^{-1}, and NO_3^--N concentrations between 0 and 546.4 mg L^{-1} (Supplementary Table 2). PNA and sole AMX systems achieved optimal efficiency when treating ammonium-rich wastewaters with low C/N ratios (C/N < 0.5) (Pan et al., 2020; Parde et al., 2025). In contrast, PDA and SNAD systems were more effective for municipal or livestock wastewaters characterized by higher C/N ratios (Chen et al., 2022). Specifically, SNAD systems operated at C/N ratios of 2.1–53.3, while PDA systems functioned at lower C/N ranges of 0.4–2.4. These results underscore the adaptability of anammox-driven technologies to diverse wastewater matrices and nitrogen loading regimes, highlighting their potential for tailored applications across livestock and municipal treatment scenarios.

3.2. Microbial communities associated with nitrogen removal

Following quality control, we obtained 1,087.96 Gb of metagenomic data and 702.7 Gb of metatranscriptomic data, enabling the identification of 18,231,823 ORFs from all assemblies. Microbial communities driving nitrification, anammox, and denitrification—the three core nitrogen removal pathways—were characterized through phylogenetic analyses of AmoA (ammonia monooxygenase), HzsA (hydrazine synthase), NirK and NirS sequences, respectively (Fig. 2, Supplementary Fig. 1, Supplementary Fig. 3 and Supplementary Fig. 4). These analyses revealed intricate microbial interactions governing nitrogen removal efficiency, N_2O emissions, and mitigation strategies in anammox-driven systems.

Anammox bacteria detected in freshwater bioreactors included *Candidatus* (*Ca.*) Brocadia, *Ca.* Jettenia, *Ca.* Kuenenia, and *Ca.* Loosdrechtia, while *Ca.* Scalindua dominated saline systems (Supplementary Fig. 1a). Notably, *Ca.* Loosdrechtia, a novel genus, was recently identified in a granular activated carbon (GAC) biofilm system treating landfill leachate (Yang et al., 2022). *Ca.* Brocadia and *Ca.* Kuenenia predominated in freshwater systems, exhibiting contrasting ecological strategies *Ca.* Brocadia (r-strategist) displayed low substrate affinity but high growth rates, whereas *Ca.* Kuenenia (k-strategist) exhibited high substrate affinity and slow growth (Oshiki et al., 2016b). Consistent with this, *Ca.* Brocadia thrived in systems with elevated NH_4^+ and NO_2^- loading rates (Supplementary Fig. 2a and Supplementary Table 2). No significant preference for suspended sludge versus biofilm growth was observed among anammox taxa, suggesting aggregate type does not drive niche partitioning of anammox bacterial community in these consortia.

Nitrification, the aerobic oxidation of ammonia to nitrite by ammonia-oxidizing archaea (AOA) and AOB, and nitrate by nitrite oxidizing bacteria (NOB) plays a pivotal role in PNA and SNAD systems. While traditional nitrification requires microbial syntrophy, complete ammonia oxidizers (comammox), exemplified by Nitrospira, can catalyze both steps independently (Daims et al., 2015). In aerobic reactors, AOB *Nitrosomonas* dominated nitrifying communities (Supplementary Fig. 1b), whereas comammox bacteria *Nitrospira* and AOA *Nitrososphaerota* were exclusively detected in TWS treating landfill leachate (Supplementary Fig. 2b). The scarcity of AOA in WWTPs may reflect copper limitation caused by organic ligand complexation (Gwak et al., 2020). Comammox bacteria, however, adapt to oligotrophic and dynamic environments (i.e., low NH_4^+ or low DO) (Dimitri Kits et al., 2017). Among AOB, *N.* europaeae/*N.* mobilis emerged as the most abundant and active clade (Supplementary Fig. 1b and Supplementary Fig. 2b), leveraging high growth rates and low substrate affinity to dominate ammonium-rich systems (Koops and Pommerening-Röser, 2001).

Denitrification biomarkers, NirK and NirS, revealed distinct taxonomic distributions of diverse denitrifiers. NirK-dependent denitrifiers spanned *Proteobacteria*, *Bacteroidota*, *Chloroflexota*, and seven other phyla, whereas NirS-dependent denitrifiers were largely restricted to *Chloroflexota* and *Proteobacteria* (Supplementary Fig. 3). This disparity likely stems from evolutionary constraints: NirS maturation involves a multi-gene operon with at least three or four subunits, while NirK maturation does not require additional subunit genes and exhibits higher mutation rates (Helen et al., 2016).

N_2O serves as an intermediate in denitrification, with a portion escaping reduction to N_2, and some denitrifiers also directly produce N_2O as an end product, leading to significant N_2O emission (Pan et al., 2012). NOR catalyzes the NO reduction to N_2O, was predominantly associated with *Proteobacteria* and *Planctomycetota* in these systems (Supplementary Fig. 4a). Microbial N_2O reduction to N_2, catalyzed by NOS, represents a major sink for this potent GHG (Kuypers et al., 2018). NosZ is divided into two lineages based on the phylogenetic analysis, clade I and clade II, with the relative abundance and phylogenetic diversity of clade II NosZ positively correlating with N_2O sink capacity (Sanford et al., 2012; Jones et al., 2013). In anammox-driven systems, clade I NosZ was mainly encoded by *Proteobacteria*, while clade II NosZ organisms exhibited higher diversity and abundance (Supplementary Fig. 4b), suggesting significant N_2O sink potential through denitrification in these systems.

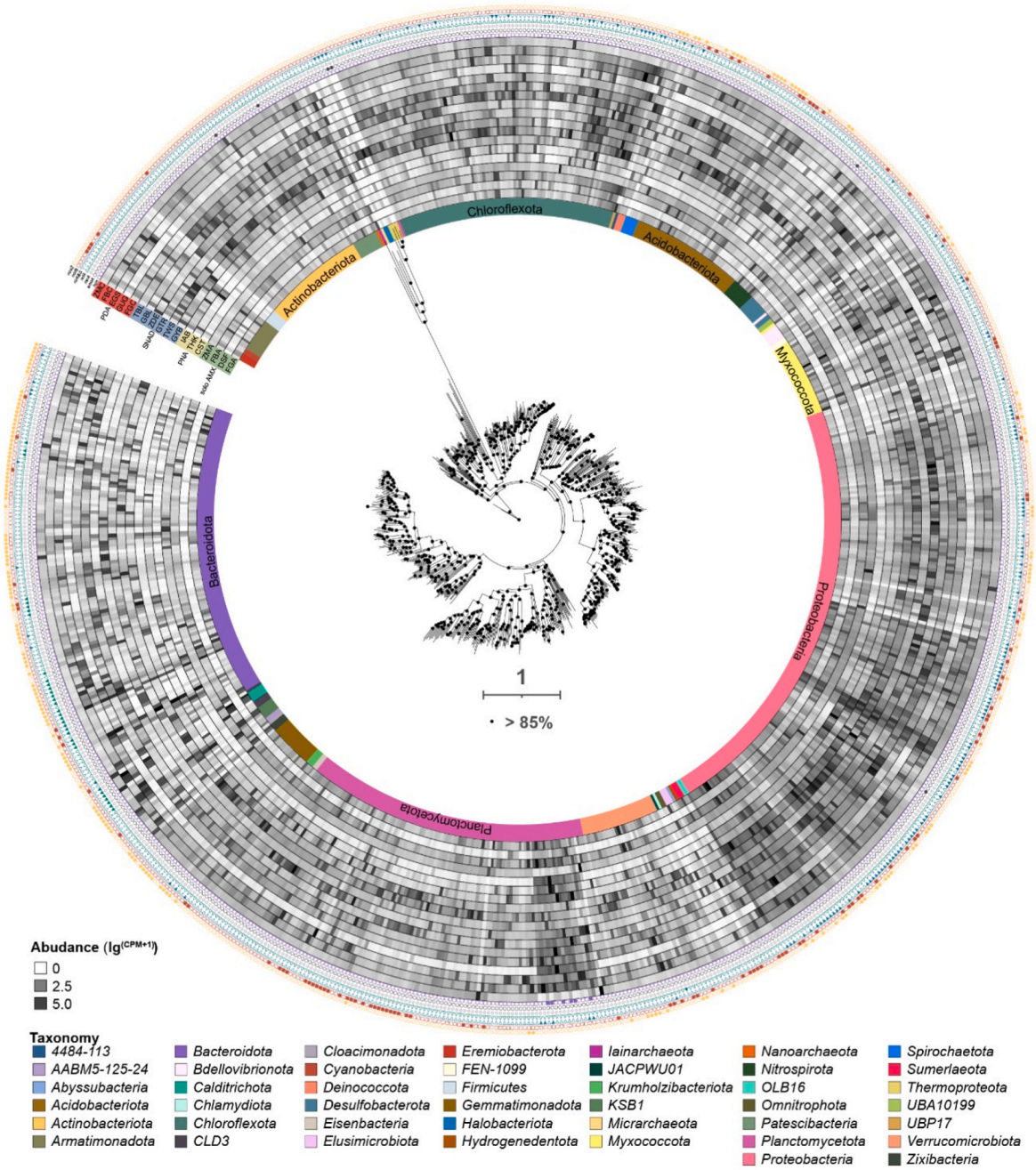

Fig. 2. Unrooted maximum likelihood trees of the 43 concatenated markers from the assembled non-redundant MAGs (average nucleotide identity >95 %) from all the studied anammox-driven systems. Different colors of the first inner cycle represent different phyla and the heatmaps of the 2–18 cycles represent genomic abundance in each sample. Different microbial nitrogen pathways were labeled by different shapes and the presence of a pathway in a MAG was indicated by the filled shape. (For interpretation of the references to color in this figure legend, the reader is referred to the Web version of this article.)

3.3. Complex nitrogen transformation networks in distinct systems

The typical sole AMX systems (DSF and FBA) were designed for the application of anammox in the second reactor of two-stage PNA systems (Guo et al., 2021; Zhuang et al., 2022). In these systems, the anammox process ($NH_4^+ + NO_2^- \rightarrow N_2$) was the dominant nitrogen removal pathway. The DSF reactor, with influent NH_4^+-N and NO_2^--N concentrations of 100 mg L^{-1}, achieved a nitrogen removal rate of 486.8 mg-N L^{-1} d^{-1}. The FBA reactor, with influent NH_4^+-N and NO_2^--N concentrations of 48.2 mg L^{-1} and 62 mg L^{-1}, respectively, maintained a nitrogen removal rate of 800 mg-N L^{-1} d^{-1}. High transcriptional levels of anammox genes were detected in both DSF (suspended sludge) and FBA (attached biofilm), indicating active anammox participated in nitrogen removal (Fig. 3). Under organic carbon-limited conditions, electrons were prioritized for NIR in the denitrification process (Pan et al., 2019). Consistently, only NIR was the only highly expressed denitrifying enzyme in these sole AMX systems, particularly in the DSF reactor, with low organic carbon (COD <120 mg L^{-1}) (Fig. 3). The highly produced NO by denitrifying NIR might be used by the highly enriched anammox bacteria as it has been proved that they can directly use NO as the sole electron acceptor for anaerobic NH_4^+ oxidation (Hu et al., 2019) and anammox activity can be stimulated by the cross-fed NO from nitrification or denitrification (Soler-Jofra et al., 2020; Zhang et al., 2024).

Two typical PNA systems (THK and IAB) were established to treat ammonium-rich wastewater with low C/N ratios (Wang et al., 2019; Soler-Jofra et al., 2020; Pan et al., 2021; Zhang et al., 2024). In these

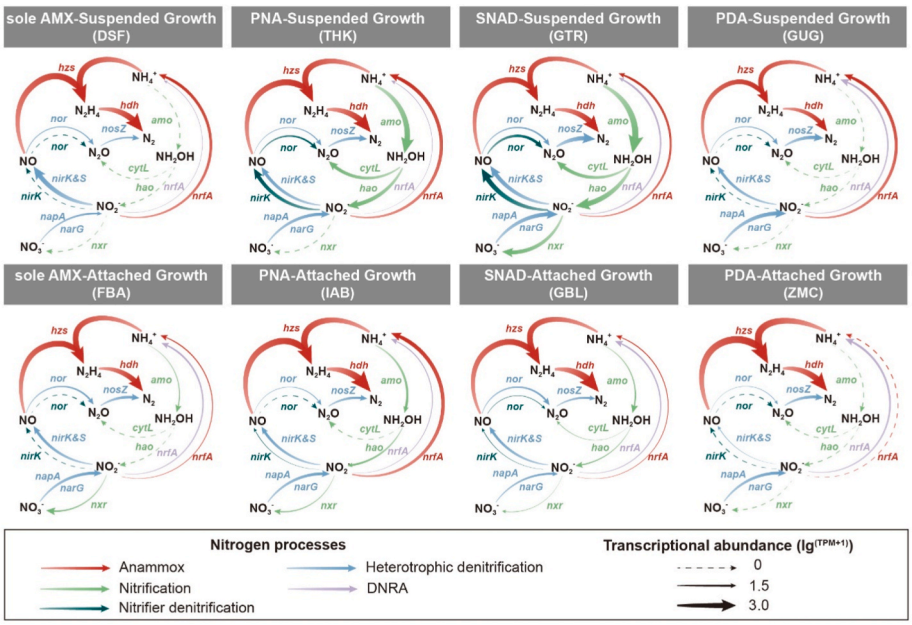

Fig. 3. The constructed microbial nitrogen cycling networks in the 8 types anammox-driven systems based on metagenomic and metatranscriptomic analyses, including AMX, PNA, SNAD, and PDA with both suspended sludge and biofilm technologies. The thickness of the line represents the gene transcriptional abundance in TPM, and different colors represent different nitrogen processes. *amo* represents ammonium monooxygenase, *hao* represents hydroxylamine oxidoreductase, *cytL* represents cytochrome P460, *nxr* represents nitrite oxidoreductase, *hzs* represents hydrazine synthase, *narG* represents respiratory nitrate reductase, *napA* represents periplasmic nitrate reductase, *nirK&S* represent NO-forming nitrite reductases, *norB* represents nitric oxide reductase, *nosZ* represents nitrous oxide reductase and *nrfA* represents cytochrome *c* nitrite reductase. (For interpretation of the references to color in this figure legend, the reader is referred to the Web version of this article.)

systems, nitrogen removal was achieved through partial-nitrification ($NH_3 \rightarrow NO_2^-$) and anammox. The influent NH_4^+-N concentrations in THK and IAB were 250 mg L^{-1} and 14.9 mg L^{-1}, respectively. Low DO levels (0.1–0.8 mg L^{-1} in THK) were maintained to achieve partial nitrification. High transcriptional levels of AMO and hydroxylamine oxidoreductase (HAO) genes in THK and IAB, particularly in THK with suspended sludge (Fig. 3), indicated efficient NH_4^+ oxidation to NO_2^- by AOB. The resulting NO_2^- and remaining NH_4^+ were simultaneously converted to N_2 by highly active anammox bacteria (Fig. 3). The rapid consumption of limited DO by AOB minimized oxygen inhibition on anammox and suppressed NOB activity, as evidenced by weak *nxr* gene transcription in IAB (Fig. 3). Additionally, comparable to the high transcriptional levels of ammonia oxidizing genes, low DO conditions (0.45 mg L^{-1} in THK) likely stimulated the transcription of *nirK* and *nor* genes related to nitrifier-denitrification (Peng et al., 2015). The accumulated NO_2^- from ammonia oxidation may also drive the expression of nitrifier-denitrification related genes for detoxification (Yu and Chandran, 2010; Brotto et al., 2018).

Two typical SNAD systems (GTR and GBL) were established to treat high C/N ratio sewage, where the nitrogen was achieved through the synergy of nitrification ($NH_3 \rightarrow NO_3^-$), anammox, and denitrification ($NO_3^- \rightarrow N_2$) in a single reactor (Fig. 3). Low DO levels (0.1 mg L^{-1} in GTR and 0.21 mg L^{-1} in GBL) were maintained to provide anoxic conditions for anammox and denitrification. High transcriptional levels of *amo*, *hao*, and *nxr* indicated strong nitrification activity in GTR (suspended sludge), whereas these levels were much lower in GBL (attached biofilm). The higher substrate diffusion efficiency in suspended sludge likely enhanced the nitrification by improving NH_4^+ and O_2 availability. In contrast, anammox gene transcription (*hzs* and *hdh*) was significantly higher in biofilm than in the suspended sludge systems, likely due to reduced substrate competition from AOB and NOB in biofilm systems. Consistent with the previous finding (Zhang et al., 2019), the relatively high C/N ratios (2.1 in GTR and 4.3 in GBL) posed a challenge for ammonium removal through anammox in SNAD systems, as denitrification is thermodynamically more favorable in the presence of sufficient organic carbon (Kumar and Lin, 2010; Daigger, 2014). Consequently, anammox genes transcription in SNAD systems with high C/N ratios were much lower than in sole AMX and PNA systems with low C/N ratios (Fig. 3).

Reactors GUG and ZMC were designed for PDA technology to treat wastewater with low COD and high NH_4^+ and NO_3^- concentrations. Nitrogen removal in these systems relied on partial-denitrification ($NO_3^- \rightarrow NO_2^-$), anammox, and dissimilatory nitrate reduction to ammonium (DNRA, $NO_3^- \rightarrow NH_4^+$) under anaerobic condition (Fig. 3). The low C/N ratios of GUG (0.4) and ZMC (0.7) provided optimal conditions for anammox technologies in treating ammonium-rich wastewater (Daigger, 2014; Lackner et al., 2014). Nitrification activity was completely inhibited by the anaerobic condition, as no nitrifying gene transcription was detected. High transcriptional levels of nitrate reductase (*napA*) and cytochrome *c* nitrite reductase (*nrfA*) genes in GUG suggested robust DNRA activity, wherein a portion of NO_3^- was reduced to NH_4^+ via NO_2^-, enhancing nitrogen removal through anammox by supplying additional substrate (Zhou et al., 2023) and reducing denitrifying activity through substrate competition (H. Wang et al., 2022).

The overall nitrogen transformation processes in four distinct anammox-driven nitrogen removal systems, including sole AMX, PNA, SNAD, and PDA, were constructed based on the presence and transcriptional levels of key nitrogen cycle related genes (Fig. 3). This synthesis reveals intricate nitrogen transformation networks across these systems, demonstrating how microbial activity, substrate availability, and operational parameters synergistically govern nitrogen removal pathways and efficiencies.

3.4. The underlaying N_2O emission mechanisms in anammox-driven systems

In hypoxic PNA and SNAD systems, the relative transcriptional levels of *amo* genes in suspended sludge (18.7 and 64.1%) were much higher than those in attached biofilms (0.3 and 1.0%) (Fig. 4), reflecting enhanced ammonia oxidation capacity in suspended biomass. NH_2OH, a

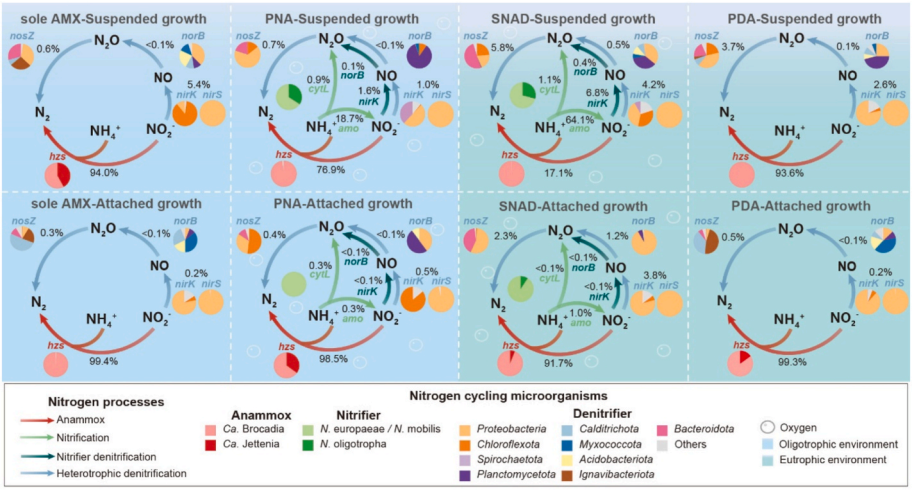

Fig. 4. The constructed microbial N_2O emission models in the 8 types of anammox-driven systems based on the relative transcriptional abundance of each gene related to N_2O metabolism. The relative contributions of different microbes contribute to each pathway was displayed by pie charts with different colors. *amo* represents ammonium monooxygenase, *hao* represents hydroxylamine oxidoreductase, *cytL* represents cytochrome P460, *nxr* represents nitrite oxidoreductase, *hzs* represents hydrazine synthase, *narG* represents respiratory nitrate reductase, *napA* represents periplasmic nitrate reductase, *nirK&S* represent NO-forming nitrite reductases, *norB* represents nitric oxide reductase, *nosZ* represents nitrous oxide reductase and *nrfA* represents cytochrome *c* nitrite reductase. (For interpretation of the references to color in this figure legend, the reader is referred to the Web version of this article.)

critical intermediate of ammonia oxidation, can leak out and abiotically react with NO_2^- to produce N_2O (Zhu-Barker et al., 2015; Soler-Jofra et al., 2021). Alternatively, NH_2OH can be biologically converted to N_2O or combined with NO to form N_2O through the NH_2OH detoxification pathway catalyzed by CytL in AOB, which is a major source of N_2O during ammonia oxidation (Caranto et al., 2016). Consistent with this, the transcriptional levels of *cytL* in suspended sludges (0.9% and 1.1%) were also higher than those in attached biofilms (0.3% and <0.1%). The varying substrate diffusion efficiencies partially explain the distinct N_2O generation potentials of nitrifiers in suspended sludge versus biofilm systems. The dense structure of biofilm likely restricts nitrifying N_2O production by limiting substrate diffusion, whereas the looser structure of suspended sludge enhances nitrifying N_2O production by facilitating rapidly diffusion of substrates from the bulk liquid to sludge core (Kragh et al., 2023).

Nitrifier denitrification ($NO_2^- \rightarrow N_2O$), catalyzed by NIR and NOR in AOB, is another significant source of N_2O in wastewater treatment systems (Shaw et al., 2006). Comparable to the stronger ammonia oxidation activities in suspended sludges, *nir* and *nor* genes exhibited higher transcriptional levels in PNA and SNAD reactors (Supplementary Fig. 5), suggesting a higher N_2O emission potential in suspended sludge compared to biofilm systems through nitrifier denitrification. Biofilms have been shown to reduce N_2O emission by 43.77 % in nitrifying integrated fixed-film activated sludge system by managing N_2O production by AOB (He et al., 2023b). Although aeration is necessary for maintaining partial nitrification in PNA and SNAD systems, DO levels are typically kept low to prevent NOB proliferation and oxygen inhibition of anammox (Yang et al., 2020, 2021; He et al., 2023b; Hu et al., 2023). Nitrifier denitrification has been found to dominate N_2O emissions under low DO conditions (<0.5 mg L^{-1}) (He et al., 2023b) and accounted for up to 73 % of the total N_2O emission in a PNA reactor with low DO levels of 0.2 mg L^{-1} (Chen et al., 2020). High NO_2^- concentrations further enhance N_2O production through nitrifier denitrification at low DO levels (<1 mg L^{-1}), while higher DO levels could reduce N_2O emissions regardless of NO_2^- levels (Peng et al., 2015), reflecting low DO combined with high NO_2^- could highly stimulate N_2O production through nitrifier denitrification. In contrast, biofilms exhibited extremely low transcriptional levels of *cytL*, *nir* and *nor* genes associated with N_2O production in AOB, along with relatively high activity of *nos* related to N_2O consumption in PNA and SNAD systems (Fig. 4), suggesting biofilms serves as effective N_2O sinks in anammox-driven systems.

The co-transcription patterns of ammonia oxidizing (*amoA* and *cytL*) and denitrifying (*nirK* and *norB*) genes in AOB were significantly correlated ($p < 0.01$) (Fig. 5), indicating a close association between ammonia oxidation and N_2O production in hypoxic anammox-driven systems (DO < 1.4 mg L^{-1}). The *nosZ/(cytL + norB)* ratio, an indicator of N_2O sink potential, showed a significantly negative relationship with *amoA* gene transcription ($p < 0.05$) (Fig. 5). Furthermore, the transcriptional activity of nitrifier *norB* exhibited a strong negative relationship with the *nosZ/(cytL + norB)* ratio ($r = -0.74$, $p < 0.01$). In contrast, denitrifing *norB* showed no significant correlation with the ratio ($p > 0.05$), underscoring the specific and stronger link of nitrifier denitrification to N_2O emission potential (Fig. 4). This finding aligns with previous studies showing that nitrifiers produce higher levels of N_2O than denitrifiers in one-stage PNA and SNAD reactors under low DO conditions (Hu et al., 2013; Ali et al., 2016).

Denitrifiers were consistently present in these anammox-driven systems but exhibit varying N_2O emission potentials. In organic carbon-limited AMX and PNA systems, transcriptional activities of denitrifying genes were generally low, with the notable exception of highly transcribed *nirK* and *nirS* (Figs. 3 and 4). Insufficient organic carbon likely prioritized NO_2^- reduction over other denitrifying steps, leading to NO accumulation (Pan et al., 2019; Liu et al., 2022). It is noteworthy that N_2O production by nitrifier denitrification could be enhanced by NO_2^- and NO accumulation in the hypoxic PNA system (Graf et al., 2014; Herrling et al., 2017). In contrast, SNAD and PDA systems, with higher organic carbon availability, greatly enhanced the transcription of denitrifying *nosZ* (up to 5.8 %) (Fig. 4), making *nosZ*--containing denitrifiers crucial N_2O sink (Conthe et al., 2019; Wan et al., 2019). Interestingly, a significant positive correlation was observed between the transcriptions of clade I *nosZ* and denitrifier *nirS* ($r = 0.87$, $p < 0.01$) but not *nirK* ($p > 0.05$) (Fig. 5). Additionally, the transcription of denitrifier clade I *nosZ* and *nirS* was positively correlated with denitrifier *norB* ($r = 0.87$, $p < 0.01$) (Fig. 5), indicating that NO_2^- reduction by *nirS*-denitrifiers is closely coupled with NO and N_2O reductions for complete denitrification. This results in lower N_2O emission potentials compared to *nirK*-denitrifiers, which are less likely to contain *nosZ* (Graf et al., 2014). These findings highlight the non-random occurrence of *nir*, *nor*, and *nos* genes in denitrifying communities and their critical role in

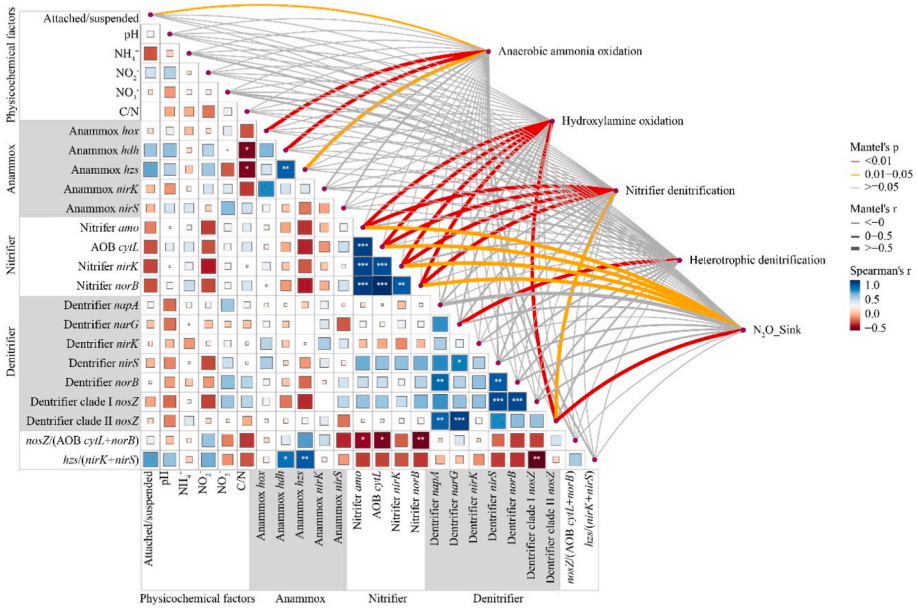

Fig. 5. Factors driving microbial nitrogen transformations and N_2O emissions in anammox-driven systems. Pairwise Spearman's correlation matrix between environmental factors and nitrogen cycle-related genes was displayed by heatmaps. Statistical significance of correlation is indicated based on false discovery rate (FDR)-adjusted p-values. The correlations between the transcriptions of nitrogen cycling processes with environmental factors and the transcriptions of nitrogen cycle genes were determined by Mantel tests. In this analysis, suspended sludge and biofilm were given the values 0 and 1, respectively.

determining the N_2O emission potentials in nitrogen removal systems.

3.5. Roles and mechanisms of biofilm in mitigating N_2O emission

Driven by multi-omics evidence indicating a higher potential for AOB-mediated N_2O production in suspended sludge-signified by the elevated transcription of key genes (e.g., *cytL* and *norB*), we hypothesized that suspended sludge would exhibit a greater N_2O emission potential than biofilm. To test this, we conducted ex-situ batch cultivation experiments comparing N_2O emission dynamics between the two biomass types from the same PNA reactor. The single-stage PNA reactor operated continuously for 740 days, during which anammox bacteria and AOB were successfully enriched in both biofilm and suspended sludge. *Ca.* Brocadia dominated the anammox bacterial communities, with a relative abundance of 8.63 % in biofilm and 14.42 % in suspended sludge, followed by *Ca.* Jettenia (7.25 % in biofilm and 3.56 % in suspended sludge). The dominant AOB, *Nitrosomonas*, had relative abundances of 1.22 % in suspended sludge and 0.33 % in biofilm (Supplementary Fig. 7).

Batch cultivation experiments were conducted to compare N_2O emission factors between biofilm and suspended sludge under low aeration condition (DO = 0.7 ± 0.2 mg L^{-1}). In the first cycle (50 min), suspended sludge consumed 1.19 mM NH_4^+-N, producing 0.62 ppmv N_2O in the headspace, while accumulating 0.02 mM NO_2^--N and 0.03 mM NO_3^--N (Fig. 6c). In contrast, the biofilm reactor produced only 0.28 ppmv N_2O after oxidizing 1.79 mM NH_4^+-N, which minimal accumulation of NO_3^--N (0.01 mM) and no detectable NO_2^--N (Fig. 6d). Similar trends were observed in subsequent cycles, with significantly higher N_2O production rates in suspended sludge compared to biofilm (Fig. 6c and d). The calculated N_2O emission factor for biofilms was 0.009 %, significantly lower than that for suspended sludge (0.025 %) ($p < 0.05$), indicating that biofilm has a lower N_2O emission potential than suspended sludge (Fig. 6e and f).

The dense structure of biofilms creates mass transfer limitations, resulting in oxygen and substance gradients (Kinh et al., 2017; Pan et al., 2019). This structural difference from biofilm underpins their potential for N_2O mitigation, as explained by mathematical models. Models based on mass balance equations link biofilm properties like thickness to DO gradients and the distribution of microbial compositions and the metabolic pathways for N_2O production and consumptions (Todt and Dörsch, 2016), while the generalized Fulazzaky approach quantities the impact of internal and external mass transfer on substrate diffusion (Hong et al., 2025). Dissolved oxygen and substrate gradients establish distinct microbial zones within the biofilm, leading to spatially segregated microbial communities and metabolic pathways for N_2O production and consumption (He et al., 2023a). As a result, nitrifiers in suspended sludge have easier access to NH_4^+ and O_2 from the bulk liquid, leading to a higher nitrification activity and accumulation of nitrogen oxide intermediates. This is evidenced by the significantly higher NO_2^- accumulation rate (ΔNO_2^--N/ΔNH_4^+-N) in suspended sludge compared to biofilm ($p < 0.05$) (Fig. 6e). Since NO_2^- is a precursor of N_2O, its accumulation is positively correlated with N_2O emissions (Tallec et al., 2006; Kim et al., 2010; Wunderlin et al., 2013). The heterogeneous distribution of microorganisms in biofilm further contributes to N_2O mitigation. In biofilms, anammox and denitrifying bacteria are concentrated in the inner layer, while a thin layer of nitrifier resides on the surface (Pan et al., 2019). In contrast, nitrifier and anammox bacteria are more uniformly distributed in suspended sludge, usually with higher nitrifier abundance (Supplementary Fig. 7) (Wells et al., 2017). The substrate diffusion gradients in biofilm extended the residence time of nitrogen oxides, allowing then to be effectively consumed by microbes within the biofilm (Pan et al., 2019). Anammox bacteria, in particular, can directly utilize external NO and NH_2OH, key precursors of N_2O, as electron acceptors for NH_4^+ oxidation (Oshiki et al., 2016b; Hu et al., 2019). Consequently, the high abundance of active anammox bacteria in biofilm reduces the N_2O emission by efficiently scavenging leaked NO and NH_2OH from nitrification and denitrification processes (Fig. 4 and Supplementary Fig. 5). In contrast, the loose structure of suspended sludge, combined with a lower abundance of anammox bacteria, resulting in higher N_2O production caused by the accumulation of nitrogen oxides (Wells et al., 2017). These findings illustrate the critical role of biofilm in mitigating N_2O emissions in anammox-driven systems, emphasizing the importance of microbial community structure and substrate diffusion dynamics in controlling N_2O production and consumption.

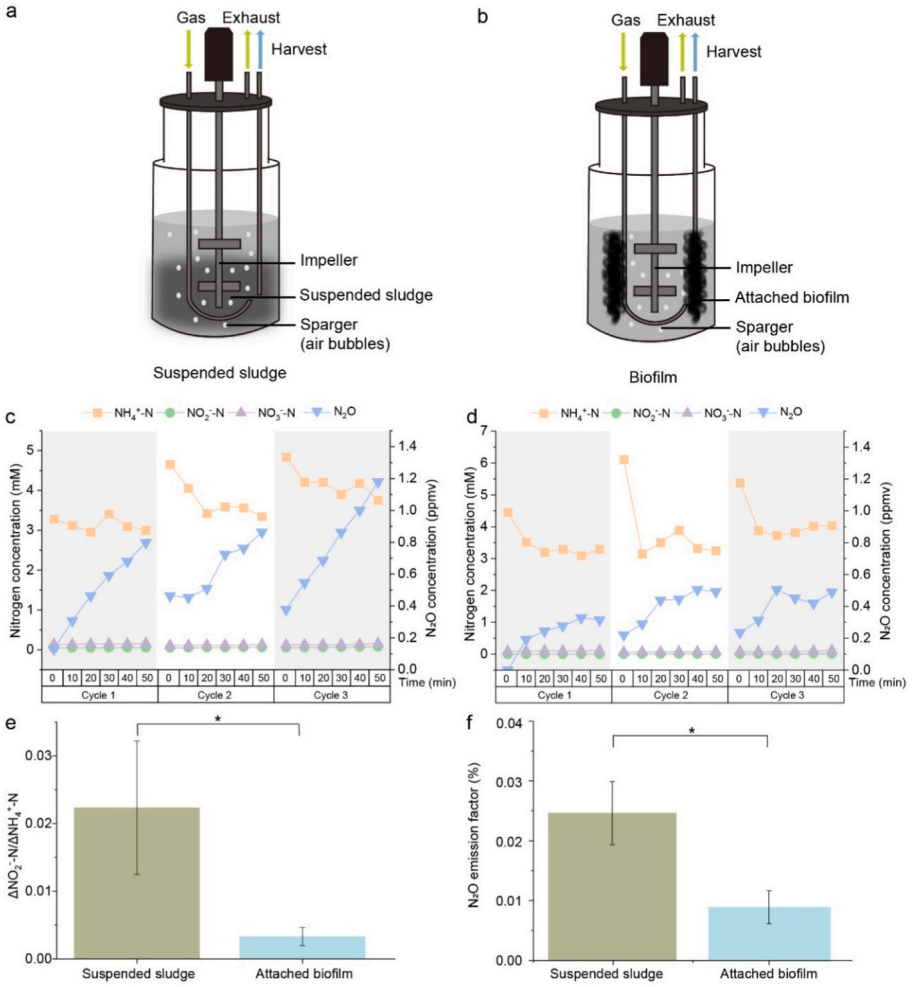

Fig. 6. Schematic illustrations of the experimental setups for suspended sludge (a) and attached biofilm (b) sampled from the same PNA reactor during batch cultivation. Panels (c) and (d) depict temporal variations in ammonium, nitrite, and nitrate concentrations, alongside gas-phase N_2O production profiles for suspended sludge and biofilm systems, respectively. Comparative analyses of the ΔNO_2^--N/ΔNH_4^+-N ratio (e) and N_2O emission factor (f) between suspended sludge and biofilm are presented, with error bars indicating standard deviations derived from triplicate biological replicates (n = 3). Statistical significance of differences was assessed using Student's t-tests (*, $p < 0.05$).

4. Conclusion and implication

This study integrated multi-omics analyses with batch cultivation experiments to elucidate the key mechanisms governing N_2O emissions in anammox-driven wastewater treatment systems. The findings demonstrate that nitrifying microorganisms, particularly AOB, serve as the primary contributors to N_2O emissions in PNA and SNAD systems under low-aeration conditions. Elevated transcriptional activities of genes involved in nitrifier denitrification pathways appear correlated with increased N_2O production observed in these systems. In contrast, strictly anaerobic configurations such as sole AMX and PDA systems exhibited significantly suppressed N_2O emissions due to limited nitrifier activity.

Biofilm-based systems demonstrated a substantial advantage in mitigating N_2O emissions, showing a 2.78-fold reduction compared to suspended sludge configurations. This mitigation effect stems primarily from the physical structure of biofilms, which creates substrate diffusion gradients that limit nitrite accumulation and enhance the scavenging of N_2O precursors by anammox bacteria. The restricted substrate transfer within biofilms reduces nitrifier activity while promoting the consumption of nitrogen oxide intermediates, thereby minimizing N_2O formation potential.

These results highlight the critical importance of microbial community structure and mass transfer dynamics in controlling greenhouse gas emissions from wastewater treatment processes. The demonstrated efficacy of biofilm systems provides a sustainable framework for designing nitrogen removal technologies that align with climate change mitigation goals. By optimizing reactor configurations to leverage these natural mitigation mechanisms, wastewater treatment facilities can achieve both operational efficiency and environmental sustainability, contributing meaningfully to global efforts in reducing anthropogenic greenhouse gas emissions.

CRediT authorship contribution statement

Zhiman Lin: Data curation, Formal analysis, Investigation, Methodology, Writing – original draft, Writing – review & editing. **Jinfan Zhang:** Data curation, Formal analysis, Methodology, Writing – original draft, Writing – review & editing. **Ru Wang:** Data curation, Software, Writing – original draft. **Jingmin Ou:** Formal analysis, Investigation, Resources. **He Zhang:** Data curation, Formal analysis. **Zihua Wang:** Data curation, Formal analysis. **Fangyuan Zheng:** Formal analysis, Resources. **Xiantao Sun:** Data curation, Software. **Xin Wei:** Investigation, Resources. **Yiming Huang:** Investigation, Resources. **Zhenguo Chen:** Methodology, Resources. **Mark C.M. van Loosdrecht:** Supervision, Writing – review & editing. **Yuchun Yang:** Funding acquisition, Methodology, Project administration, Supervision, Writing – original draft, Writing – review & editing.

Declaration of competing interest

The authors declare that they have no known competing financial interests or personal relationships that could have appeared to influence the work reported in this paper.

Acknowledgements

This study was funded by Natural Science Foundation of China (grant no. 32470097, 32100086), Guangdong Provincial Field Observation and Research Station for Biodiversity and Biotic Interactions in Chebaling Lingnan Mountain Forests (grant no. 2025B1212050003), and the 2025 Guangdong Provincial Dedicated Funds for State Key Laboratories.

Appendix A. Supplementary data

Supplementary data to this article can be found online at https://doi.org/10.1016/j.ibiod.2025.106274.

Data availability

The raw 16S rRNA sequencing data, reactor performance data, and analysis scripts have been deposited in the Figshare repository and are available under the accession code 10.6084/m9.figshare.30398905.

References

Ali, M., Rathnayake, R.M.L.D., Zhang, L., Ishii, S., Kindaichi, T., Satoh, H., Toyoda, S., Yoshida, N., Okabe, S., 2016. Source identification of nitrous oxide emission pathways from a single-stage nitritation-anammox granular reactor. Water Res. 102, 147–157. https://doi.org/10.1016/j.watres.2016.06.034.

Alneberg, J., Bjarnason, B.S., De Bruijn, I., Schirmer, M., Quick, J., Ijaz, U.Z., Lahti, L., Loman, N.J., Andersson, A.F., Quince, C., 2014. Binning metagenomic contigs by coverage and composition. Nat. Methods 11, 1144–1146. https://doi.org/10.1038/nmeth.3103.

Brotto, A.C., Annavajhala, M.K., Chandran, K., 2018. Metatranscriptomic investigation of adaptation in NO and N_2O production from a lab-scale nitrification process upon repeated exposure to anoxic-aerobic cycling. Front. Microbiol. 9, 1–15. https://doi.org/10.3389/fmicb.2018.03012.

Cao, Y., van Loosdrecht, M.C.M., Daigger, G.T., 2017. Mainstream partial nitritation–anammox in municipal wastewater treatment: status, bottlenecks, and further studies. Appl. Microbiol. Biotechnol. 101, 1365–1383. https://doi.org/10.1007/s00253-016-8058-7.

Capella-Gutiérrez, S., Silla-Martínez, J.M., Gabaldón, T., 2009. trimAl: a tool for automated alignment trimming in large-scale phylogenetic analyses. Bioinformatics 25, 1972–1973. https://doi.org/10.1093/bioinformatics/btp348.

Caporaso, J.G., Kuczynski, J., Stombaugh, J., Bittinger, K., Bushman, F.D., Costello, E.K., Fierer, N., Peña, A.G., Goodrich, J.K., Gordon, J.I., Huttley, G.A., Kelley, S.T., Knights, D., Koenig, J.E., Ley, R.E., Lozupone, C.A., Mcdonald, D., Muegge, B.D., Pirrung, M., Reeder, J., Sevinsky, J.R., Turnbaugh, P.J., Walters, W.A., Widmann, J., Yatsunenko, T., Zaneveld, J., Knight, R., 2010. Correspondence QIIME allows analysis of high- throughput community sequencing data intensity normalization improves color calling in SOLiD sequencing. Nat. Publ. Gr. 7, 335–336. https://doi.org/10.1038/nmeth0510-335.

Caranto, J.D., Vilbert, A.C., Lancaster, K.M., 2016. Nitrosomonas europaea cytochrome P460 is a direct link between nitrification and nitrous oxide emission. Proc. Natl. Acad. Sci. U. S. A 113, 14704–14709. https://doi.org/10.1073/pnas.1611051113.

Chaumeil, P.A., Mussig, A.J., Hugenholtz, P., Parks, D.H., 2020. GTDB-Tk: a toolkit to classify genomes with the genome taxonomy database. Bioinformatics 36, 1925–1927. https://doi.org/10.1093/bioinformatics/btz848.

Chen, G., Zhang, Y., Wang, X., Chen, F., Lin, L., Ruan, Q., Wang, Y., Wang, F., Cao, W., Chiang, P., 2020. Optimizing of operation strategies of the single-stage partial nitrification-anammox process. J. Clean. Prod. 256, 120667. https://doi.org/10.1016/j.jclepro.2020.120667.

Chen, Y., Guo, G., Li, Y.Y., 2022. A review on upgrading of the anammox-based nitrogen removal processes: performance, stability, and control strategies. Bioresour. Technol. 364, 127992. https://doi.org/10.1016/j.biortech.2022.127992.

Conthe, M., Lycus, P., Arntzen, M., Ramos da Silva, A., Frostegård, Å., Bakken, L.R., Kleerebezem, R., van Loosdrecht, M.C.M., 2019. Denitrification as an N_2O sink. Water Res. 151, 381–387. https://doi.org/10.1016/j.watres.2018.11.087.

Daigger, G.T., 2014. Oxygen and carbon requirements for biological nitrogen removal processes accomplishing nitrification, nitritation, and anammox. Water Environ. Res. 86, 204–209. https://doi.org/10.2175/106143013x13807328849459.

Daims, H., Lebedeva, E.V., Pjevac, P., Han, P., Herbold, C., Albertsen, M., Jehmlich, N., Palatinszky, M., Vierheilig, J., Bulaev, A., Kirkegaard, R.H., Von Bergen, M., Rattei, T., Bendinger, B., Nielsen, P.H., Wagner, M., 2015. Complete nitrification by Nitrospira bacteria. Nature 528, 504–509. https://doi.org/10.1038/nature16461.

Debeljak, P., Bayer, B., Sun, Y., Herndl, G.J., Obernosterer, I., 2023. Seasonal patterns in microbial carbon and iron transporter expression in the Southern Ocean. Microbiome 11, 1–12. https://doi.org/10.1186/s40168-023-01600-3.

Dimitri Kits, K., Sedlacek, C.J., Lebedeva, E.V., Han, P., Bulaev, A., Pjevac, P., Daebeler, A., Romano, S., Albertsen, M., Stein, L.Y., Daims, H., Wagner, M., 2017. Kinetic analysis of a complete nitrifier reveals an oligotrophic lifestyle. Nature 549, 269–272. https://doi.org/10.1038/nature23679.

Eggleston, S., Buendia, L.M.K., 2006. IPCC guidelines for national greenhouse gas inventories: intergovernmental panel on climate change. Institute for Global Environmental Strategies.

Fernández, I., Vázquez-Padín, J.R., Mosquera-Corral, A., Campos, J.L., Méndez, R., 2008. Biofilm and granular systems to improve anammox biomass retention. Biochem. Eng. J. 42, 308–313. https://doi.org/10.1016/j.bej.2008.07.011.

Forster, D., Dunthorn, M., Stoeck, T., Mahé, F., 2016. Comparison of three clustering approaches for detecting novel environmental microbial diversity. PeerJ. https://doi.org/10.7717/peerj.1692, 2016.

Graf, D.R.H., Jones, C.M., Hallin, S., 2014. Intergenomic comparisons highlight modularity of the denitrification pathway and underpin the importance of community structure for N_2O emissions. PLoS One 9, 1–20. https://doi.org/10.1371/journal.pone.0114118.

Guo, Y., Zhao, Y., Tang, X., Na, T., Pan, J., Zhao, H., Liu, S., 2021. Deciphering bacterial social traits via diffusible signal factor (DSF) -mediated public goods in an anammox community. Water Res. 191, 116802. https://doi.org/10.1016/j.watres.2020.116802.

Gwak, J.H., Jung, M.Y., Hong, H., Kim, J.G., Quan, Z.X., Reinfelder, J.R., Spasov, E., Neufeld, J.D., Wagner, M., Rhee, S.K., 2020. Archaeal nitrification is constrained by copper complexation with organic matter in municipal wastewater treatment plants. ISME J. 14, 335–346. https://doi.org/10.1038/s41396-019-0538-1.

He, Y., Liu, Yingrui, Li, X., Zhu, T., Liu, Yiwen, 2023a. Unveiling the roles of biofilm in reducing N2O emission in a nitrifying integrated fixed-film activated sludge (IFAS) system. Water Res. 243, 120326. https://doi.org/10.1016/j.watres.2023.120326.

He, Y., Liu, Yingrui, Li, X., Zhu, T., Liu, Yiwen, 2023b. Unveiling the roles of biofilm in reducing N_2O emission in a nitrifying integrated fixed-film activated sludge (IFAS) system. Water Res. 243, 120326. https://doi.org/10.1016/j.watres.2023.120326.

Helen, D., Kim, H., Tytgat, B., Anne, W., 2016. Highly diverse nirK genes comprise two major clades that harbour ammonium-producing denitrifiers. BMC Genom. 17, 1–13. https://doi.org/10.1186/s12864-016-2465-0.

Herrling, M.P., Weisbrodt, J., Kirkland, C.M., Williamson, N.H., Lackner, S., Codd, S.L., Seymour, J.D., Guthausen, G., Horn, H., 2017. NMR investigation of water diffusion in different biofilm structures. Biotechnol. Bioeng. 114, 2857–2867. https://doi.org/10.1002/bit.26392.

Hoang, D.T., Chernomor, O., von Haeseler, A., Minh, B.Q., Vinh, L.S., 2018. UFBoot2: improving the ultrafast bootstrap approximation. Molecular biology and evolution. Mol. Biol. Evol. 35, 518–522. https://doi.org/10.5281/zenodo.854445.

Hong, C.Y., Muda, K., Fulazzaky, M.A., 2025. Mechanisms and mass transfer kinetics of anammox during sludge enrichment. Int. Biodeterior. Biodegrad. 204, 106140. https://doi.org/10.1016/j.ibiod.2025.106140.

Hood-Nowotny, R., Umana, N.H.-N., Inselbacher, E., Oswald- Lachouani, P., Wanek, W., 2010. Alternative methods for measuring inorganic, organic, and total dissolved nitrogen in soil. Soil Sci. Soc. Am. J. 74, 1018–1027. https://doi.org/10.2136/sssaj2009.0389.

Hu, Z., Zhang, J., Li, S., Xie, H., 2013. Impact of carbon source on nitrous oxide emission from anoxic/oxic biological nitrogen removal process and identification of its emission sources. Environ. Sci. Pollut. Res. 20, 1059–1069. https://doi.org/10.1007/s11356-012-1018-6.

Hu, Z., Wessels, H.J.C.T., van Alen, T., Jetten, M.S.M., Kartal, B., 2019. Nitric oxide-dependent anaerobic ammonium oxidation. Nat. Commun. 10. https://doi.org/10.1038/s41467-019-09268-w.

Hu, P., Qian, Y., Liu, J., Gao, L., Li, Y., Xu, Y., Wu, J., Hong, Y., Ford, T., Radian, A., Yang, Y., Gu, J.D., 2023. Delineation of the complex microbial nitrogen-transformation network in an anammox-driven full-scale wastewater treatment plant. Water Res. 235, 119799. https://doi.org/10.1016/j.watres.2023.119799.

Huws, S.A., Edwards, J.E., Kim, E.J., Scollan, N.D., 2007. Specificity and sensitivity of eubacterial primers utilized for molecular profiling of bacteria within complex microbial ecosystems. J. Microbiol. Methods 70, 565–569. https://doi.org/10.1016/j.mimet.2007.06.013.

Hyatt, Doug, Chen, Gwo-Liang, LoCascio, Philip F., Miriam, L Land, Frank W Larimer, L. J.H., 2010. Integrated nr database in protein annotation system and its localization. Nat. Commun. 6, 1–8.

Jones, C.M., Graf, D.R.H., Bru, D., Philippot, L., Hallin, S., 2013. The unaccounted yet abundant nitrous oxide-reducing microbial community: a potential nitrous oxide sink. ISME J. 7, 417–426. https://doi.org/10.1038/ismej.2012.125.

Kalyaanamoorthy, S., Minh, B.Q., Wong, T.K.F., Von Haeseler, A., Jermiin, L.S., 2017. ModelFinder: fast model selection for accurate phylogenetic estimates. Nat. Methods 14, 587–589. https://doi.org/10.1038/nmeth.4285.

Kang, D.D., Froula, J., Egan, R., Wang, Z., 2015. MetaBAT, an efficient tool for accurately reconstructing single genomes from complex microbial communities. PeerJ 1–15. https://doi.org/10.7717/peerj.1165, 2015.

Kim, S.W., Miyahara, M., Fushinobu, S., Wakagi, T., Shoun, H., 2010. Nitrous oxide emission from nitrifying activated sludge dependent on denitrification by ammonia-oxidizing bacteria. Bioresour. Technol. 101, 3958–3963. https://doi.org/10.1016/j.biortech.2010.01.030.

Kinh, C.T., Suenaga, T., Hori, T., Riya, S., Hosomi, M., Smets, B.F., Terada, A., 2017. Counter-diffusion biofilms have lower N_2O emissions than co-diffusion biofilms during simultaneous nitrification and denitrification: insights from depth-profile analysis. Water Res. 124, 363–371. https://doi.org/10.1016/j.watres.2017.07.058.

Konstantinidis, K.T., Tiedje, J.M., 2005. Genomic insights that advance the species definition for prokaryotes. Proc. Natl. Acad. Sci. U. S. A 102, 2567–2572. https://doi.org/10.1073/pnas.0409727102.
Koops, H.P., Pommerening-Röser, A., 2001. Distribution and ecophysiology of the nitrifying bacteria emphasizing cultured species. FEMS Microbiol. Ecol. 37, 1–9. https://doi.org/10.1016/S0168-6496(01)00137-4.
Kopylova, E., Noé, L., Touzet, H., 2012. SortMeRNA: fast and accurate filtering of ribosomal RNAs in metatranscriptomic data. Bioinformatics 28, 3211–3217. https://doi.org/10.1093/bioinformatics/bts611.
Kragh, K.N., Tolker-Nielsen, T., Lichtenberg, M., 2023. The non-attached biofilm aggregate. Commun. Biol. 6, 1–13. https://doi.org/10.1038/s42003-023-05281-4.
Kumar, M., Lin, J.G., 2010. Co-existence of anammox and denitrification for simultaneous nitrogen and carbon removal-strategies and issues. J. Hazard. Mater. 178, 1–9. https://doi.org/10.1016/j.jhazmat.2010.01.077.
Kuypers, M.M.M., Marchant, H.K., Kartal, B., 2018. The microbial nitrogen-cycling network. Nat. Rev. Microbiol. 16, 263–276. https://doi.org/10.1038/nrmicro.2018.9.
Kyung, D., Kim, M., Chang, J., Lee, W., 2015. Estimation of greenhouse gas emissions from a hybrid wastewater treatment plant. J. Clean. Prod. 95, 117–123. https://doi.org/10.1016/j.jclepro.2015.02.032.
Lackner, S., Gilbert, E.M., Vlaeminck, S.E., Joss, A., Horn, H., van Loosdrecht, M.C.M., 2014. Full-scale partial nitritation/anammox experiences - an application survey. Water Res. 55, 292–303. https://doi.org/10.1016/j.watres.2014.02.032.
Langmead, B., Salzberg, S.L., 2012. Fast gapped-read alignment with bowtie 2. Nat. Methods 9, 357–359. https://doi.org/10.1038/nmeth.1923.
Letunic, I., Bork, P., 2019. Interactive tree of life (iTOL) v4: recent updates and new developments. Nucleic Acids Res. 47, 256–259. https://doi.org/10.1093/nar/gkz239.
Liang, Y., Gao, P., Jiao, Y., Zhang, Z., Xin, Y., Xia, W., Gu, J.D., 2025. Dinitrogen production modes of diverse anammox bacteria and the contribution in nitrogen cycle: a review. Int. Biodeterior. Biodegrad. 203, 106113. https://doi.org/10.1016/j.ibiod.2025.106113.
Lin, Z., Ma, K., Yang, Y., 2022. Nitrous oxide emission from full-scale Anammox-driven wastewater treatment systems. Life 12. https://doi.org/10.3390/life12070971.
Liu, Yiwen, Liu, Yingrui, He, Y., Ren, S., Zhu, T., 2022. Selective organic carbon enrichment influences nitrous oxide reduction by denitrifiers: electron competition insights. ACS ES&T Water 2, 1265–1275. https://doi.org/10.1021/acsestwater.2c00161.
Ma, C., Jensen, M.M., Smets, B.F., Thamdrup, B., 2017. Pathways and controls of N_2O production in nitritation-Anammox biomass. Environ. Sci. Technol. 51, 8981–8991. https://doi.org/10.1021/acs.est.7b01225.
Miranda, K.M., Espey, M.G., Wink, D.A., 2001. A rapid, simple spectrophotometric method for simultaneous detection of nitrate and nitrite. Nitric Oxide - Biol. Chem. 5, 62–71. https://doi.org/10.1006/niox.2000.0319.
Nguyen, L.T., Schmidt, H.A., Von Haeseler, A., Minh, B.Q., 2015. IQ-TREE: a fast and effective stochastic algorithm for estimating maximum-likelihood phylogenies. Mol. Biol. Evol. 32, 268–274. https://doi.org/10.1093/molbev/msu300.
Olm, M.R., Brown, C.T., Brooks, B., Banfield, J.F., 2017. DRep: a tool for fast and accurate genomic comparisons that enables improved genome recovery from metagenomes through de-replication. ISME J. 11, 2864–2868. https://doi.org/10.1038/ismej.2017.126.
Oshiki, M., Ali, M., Shinyako-Hata, K., Satoh, H., Okabe, S., 2016a. Hydroxylamine-dependent anaerobic ammonium oxidation (anammox) by "Candidatus Brocadia sinica.". Environ. Microbiol. 18, 3133–3143. https://doi.org/10.1111/1462-2920.13355.
Oshiki, M., Satoh, H., Okabe, S., 2016b. Ecology and physiology of anaerobic ammonium oxidizing bacteria. Environ. Microbiol. 18, 2784–2796. https://doi.org/10.1111/1462-2920.13134.
Pan, Y., Ye, L., Ni, B.J., Yuan, Z., 2012. Effect of pH on N_2O reduction and accumulation during denitrification by methanol utilizing denitrifiers. Water Res. 46, 4832–4840. https://doi.org/10.1016/j.watres.2012.06.003.
Pan, Y., Liu, Y., Peng, L., Ngo, H.H., Guo, W., Wei, W., Wang, D., Ni, B.J., 2019. Substrate diffusion within biofilms significantly influencing the electron competition during denitrification. Environ. Sci. Technol. 53, 261–269. https://doi.org/10.1021/acs.est.8b05476.
Pan, Z., Dai, R., Liao, J., Lin, J.G., Hong, Y., Ling, J., Xu, Y., Li, Y., Peng, J., 2020. Spontaneous formation and mechanism of anaerobic ammonium oxidation (anammox) bacteria in swine wastewater treatment system. Int. Biodeterior. Biodegrad. 154, 105058. https://doi.org/10.1016/j.ibiod.2020.105058.
Pan, J., Huo, T., Yang, H., Li, Z., Chen, L., Niu, Z., Ni, S., Liu, S., 2021. Metabolic patterns reveal enhanced anammox activity at low nitrogen conditions in the integrated I-ABR. Water Environ. Res. 93, 1455–1465. https://doi.org/10.1002/wer.1511.
Parde, D., Singh, A., Behera, M., Dash, R.R., 2025. Substrate dynamics on anammox inhibition during domestic wastewater treatment under controlled and ambient temperature. Int. Biodeterior. Biodegrad. 204, 106158. https://doi.org/10.1016/j.ibiod.2025.106158.
Parks, D.H., Imelfort, M., Skennerton, C.T., Hugenholtz, P., Tyson, G.W., 2015. CheckM: assessing the quality of microbial genomes recovered from isolates, single cells, and metagenomes. Genome Res. 25, 1043–1055. https://doi.org/10.1101/gr.186072.114.
Peng, L., Ni, B.J., Ye, L., Yuan, Z., 2015. The combined effect of dissolved oxygen and nitrite on N_2O production by ammonia oxidizing bacteria in an enriched nitrifying sludge. Water Res. 73, 29–36. https://doi.org/10.1016/j.watres.2015.01.021.
Quast, C., Pruesse, E., Yilmaz, P., Gerken, J., Schweer, T., Yarza, P., Peplies, J., Glöckner, F.O., 2013. The SILVA ribosomal RNA gene database project: improved data processing and web-based tools. Nucleic Acids Res. 41, 590–596. https://doi.org/10.1093/nar/gks1219.
Pachaur, Rajendra K., Allen, Myles R., Barros, Vicente R., Broome, John, Cramer, Wolfgang, Christ, Renate, Church, John A., Clarke, Leon, Dahe, Qin, Da, Purnamita, van Y, J.-P., Technical, 2014. Climate change 2014: synthesis report. In: contribution of working groups I, II and III to the fifth assessment report of the intergovermental panel on cimate change, The ANNALS of the American Academy of Political and Social Science.
Sanford, R.A., Wagner, D.D., Wu, Q., Chee-Sanford, J.C., Thomas, S.H., Cruz-García, C., Rodríguez, G., Massol-Deyá, A., Krishnani, K.K., Ritalahti, K.M., Nissen, S., Konstantinidis, K.T., Löffler, F.E., 2012. Unexpected nondenitrifier nitrous oxide reductase gene diversity and abundance in soils. Proc. Natl. Acad. Sci. U. S. A 109, 19709–19714. https://doi.org/10.1073/pnas.1211238109.
Segata, N., Waldron, L., Ballarini, A., Narasimhan, V., Jousson, O., Huttenhower, C., 2012. Metagenomic microbial community profiling using unique clade-specific marker genes. Nat. Methods 9, 811–814. https://doi.org/10.1038/nmeth.2066.
Shaw, L.J., Nicol, G.W., Smith, Z., Fear, J., Prosser, J.I., Baggs, E.M., 2006. Nitrosospira spp. can produce nitrous oxide via a nitrifier denitrification pathway. Environ. Microbiol. 8, 214–222. https://doi.org/10.1111/j.1462-2920.2005.00882.x.
Soler-Jofra, A., Laureni, M., Warmerdam, M., Pérez, J., van Loosdrecht, M.C.M., 2020. Hydroxylamine metabolism of Ca. Kuenenia stuttgartiensis. Water Res. 184. https://doi.org/10.1016/j.watres.2020.116188.
Soler-Jofra, A., Pérez, J., van Loosdrecht, M.C.M., 2021. Hydroxylamine and the nitrogen cycle: a review. Water Res. 190, 116723. https://doi.org/10.1016/j.watres.2020.116723.
Tallec, G., Garnier, J., Billen, G., Gousailles, M., 2006. Nitrous oxide emissions from secondary activated sludge in nitrifying conditions of urban wastewater treatment plants: effect of oxygenation level. Water Res. 40, 2972–2980. https://doi.org/10.1016/j.watres.2006.05.037.
Todt, D., Dörsch, P., 2016. Mechanism leading to N_2O production in wastewater treating biofilm systems. Rev. Environ. Sci. Biotechnol. 15, 355–378. https://doi.org/10.1007/s11157-016-9401-2.
Uritskiy, G.V., DiRuggiero, J., Taylor, J., 2018. MetaWRAP—a flexible pipeline for genome-resolved metagenomic data analysis. Microbiome 6, 1–25. https://doi.org/10.1186/s40168-018-0541-1.
Wan, X., Baeten, J.E., Volcke, E.I.P., 2019. Effect of operating conditions on N2O emissions from one-stage partial nitritation-anammox reactors. Biochem. Eng. J. 143, 24–33. https://doi.org/10.1016/j.bej.2018.12.004.
Wang, Yulin, Niu, Q., Zhang, X., Liu, L., Wang, Yubo, Chen, Y., Negi, M., Figeys, D., Li, Y. Y., Zhang, T., 2019. Exploring the effects of operational mode and microbial interactions on bacterial community assembly in a one-stage partial-nitritation anammox reactor using integrated multi-omics. Microbiome 7, 1–15. https://doi.org/10.1186/s40168-019-0730-6.
Wang, H., Chen, C., Yang, E., Tu, Z., Liang, J., Dai, X., Chen, H., 2022. Revealing the effect of biofilm formation in partial nitritation-anammox systems: start-up, performance stability, and recovery. Bioresour. Technol. 357, 127379. https://doi.org/10.1016/j.biortech.2022.127379.
Wang, W., Wang, T., Liu, Q., Wang, H., Xue, H., Zhang, Z., Wang, Y., 2022. Biochar-mediated DNRA pathway of anammox bacteria under varying COD/N ratios. Water Res. 212, 118100. https://doi.org/10.1016/j.watres.2022.118100.
Wells, G.F., Shi, Y., Laureni, M., Rosenthal, A., Szivák, I., Weissbrodt, D.G., Joss, A., Buergmann, H., Johnson, D.R., Morgenroth, E., 2017. Comparing the resistance, resilience, and stability of replicate moving bed biofilm and suspended growth combined nitritation-Anammox reactors. Environ. Sci. Technol. 51, 5108–5117. https://doi.org/10.1021/acs.est.6b05878.
Wu, Y.W., Simmons, B.A., Singer, S.W., 2016. MaxBin 2.0: an automated binning algorithm to recover genomes from multiple metagenomic datasets. Bioinformatics 32, 605–607. https://doi.org/10.1093/bioinformatics/btv638.
Wu, L., Peng, L., Wei, W., Wang, D., Ni, B.J., 2020. Nitrous oxide production from wastewater treatment: the potential as energy resource rather than potent greenhouse gas. J. Hazard. Mater. 387, 121694. https://doi.org/10.1016/j.jhazmat.2019.121694.
Wunderlin, P., Lehmann, M.F., Siegrist, H., Tuzson, B., Joss, A., Emmenegger, L., Mohn, J., 2013. Isotope signatures of N_2O in a mixed microbial population system: constraints on N_2O producing pathways in wastewater treatment. Environ. Sci. Technol. 47, 1339–1348. https://doi.org/10.1021/es303174x.
Xu, Xiaoguang, Yang, Y., Zhou, Y., Ma, J., Li, J., Zhou, X., Zhao, X., Wu, F., Song, K., 2025. Global patterns and drivers of coupling between anammox and denitrification processes across inland aquatic ecosystems. Commun. Earth Environ. 6, 1–11. https://doi.org/10.1038/s43247-024-01980-w.
Xu, Xin, Zou, Y., Pan, H., Zhang, R., Gu, B., 2025. Safeguarding groundwater nitrate within regional boundaries in China. Environ. Sci. Technol. 59, 467–477. https://doi.org/10.1021/acs.est.4c08197.
Yamada, K.D., Tomii, K., Katoh, K., 2016. Application of the MAFFT sequence alignment program to large data - reexamination of the usefulness of chained guide trees. Bioinformatics 32, 3246–3251. https://doi.org/10.1093/bioinformatics/btw412.
Yang, Y., Pan, J., Zhou, Z., Wu, J., Liu, Y., Lin, J.G., Hong, Y., Li, X., Li, M., Gu, J.D., 2020. Complex microbial nitrogen-cycling networks in three distinct anammox-inoculated wastewater treatment systems. Water Res. 168, 115142. https://doi.org/10.1016/j.watres.2019.115142.
Yang, Y., Azari, M., Herbold, C.W., Li, M., Chen, H., Ding, X., Denecke, M., Gu, J.D., 2021. Activities and metabolic versatility of distinct anammox bacteria in a full-scale wastewater treatment system. Water Res. 206, 117763. https://doi.org/10.1016/j.watres.2021.117763.
Yang, Y., Lu, Z., Azari, M., Kartal, B., Du, H., Cai, M., Herbold, C.W., Ding, X., Denecke, M., Li, X., Li, M., Gu, J.D., 2022. Discovery of a new genus of anaerobic

ammonium oxidizing bacteria with a mechanism for oxygen tolerance. Water Res. 226, 119165. https://doi.org/10.1016/j.watres.2022.119165.

Yu, R., Chandran, K., 2010. Strategies of nitrosomonas europaea 19718 to counter low dissolved oxygen and high nitrite concentrations. BMC Microbiol. 10. https://doi.org/10.1186/1471-2180-10-70.

Zhang, M., Wang, S., Ji, B., Liu, Y., 2019. Towards mainstream deammonification of municipal wastewater: partial nitrification-anammox versus partial denitrification-anammox. Sci. Total Environ. 692, 393–401. https://doi.org/10.1016/j.scitotenv.2019.07.293.

Zhang, Xiaonong, Zhang, Xingxing, Chen, J., Wu, P., Yang, Z., Zhou, L., Zhu, Z., Wu, Z., Zhang, K., Wang, Y., Ruth, G., 2023. A critical review of improving mainstream anammox systems: based on macroscopic process regulation and microscopic enhancement mechanisms. Environ. Res. 236, 116770. https://doi.org/10.1016/j.envres.2023.116770.

Zhang, S., Li, C., Lv, H., Cui, B., Zhou, D., 2024. Anammox activity improved significantly by the cross-fed NO from ammonia-oxidizing bacteria and denitrifying bacteria to anammox bacteria. Water Res. 249, 120986. https://doi.org/10.1016/j.watres.2023.120986.

Zhou, L., Zhao, B., Zhuang, W.Q., 2023. Double-edged sword effects of dissimilatory nitrate reduction to ammonium (DNRA) bacteria on anammox bacteria performance in an MBR reactor. Water Res. 233, 119754. https://doi.org/10.1016/j.watres.2023.119754.

Zhu-Barker, X., Cavazos, A.R., Ostrom, N.E., Horwath, W.R., Glass, J.B., 2015. The importance of abiotic reactions for nitrous oxide production. Biogeochemistry 126, 251–267. https://doi.org/10.1007/s10533-015-0166-4.

Zhuang, J.L., Sun, X., Zhao, W.Q., Zhang, X., Zhou, J.J., Ni, B.J., Liu, Y. Di, Shapleigh, J. P., Li, W., 2022. The anammox coupled partial-denitrification process in an integrated granular sludge and fixed-biofilm reactor developed for mainstream wastewater treatment: performance and community structure. Water Res. 210, 117964. https://doi.org/10.1016/j.watres.2021.117964.